Front. Struct. Civ. Eng. 2022, 16(10): 1336–1350
https://doi.org/10.1007/s11709-022-0852-y

RESEARCH ARTICLE

Fatigue evaluation of steel-concrete composite deck in steel truss bridge——A case study

Huating CHEN[a*], Xianwei ZHAN[a], Xiufu ZHU[b], Wenxue ZHANG[a]

[a] *Faculty of Urban Construction, Beijing University of Technology, Beijing 100021, China*
[b] *Tai'an High-tech Industrial Development Zone Management Committee, Tai'an 271000, China*
[*] *Corresponding author. E-mail: chenhuating@bjut.edu.cn*

ABSTRACT An innovative composite deck system has recently been proposed for improved structural performance. To study the fatigue behavior of a steel-concrete composite bridge deck, we took a newly-constructed rail-cum-road steel truss bridge as a case study. The transverse stress history of the bridge deck near the main truss under the action of a standard fatigue vehicle was calculated using finite element analysis. Due to the fact that fatigue provision remains unavailable in the governing code of highway concrete bridges in China, a preliminary fatigue evaluation was conducted according to the fib Model Code. The results indicate that flexural failure of the bridge deck in the transverse negative bending moment region is the controlling fatigue failure mode. The fatigue life associated with the fatigue fracture of steel reinforcement is 56 years. However, while the top surface of the bridge deck concrete near the truss cracks after just six years, the bridge deck performs with fatigue cracks during most of its design service life. Although fatigue capacity is acceptable under design situations, overloading or understrength may increase its risk of failure. The method presented in this work can be applied to similar bridges for preliminary fatigue assessment.

KEYWORDS Fatigue assessment, composite bridge deck, rail-cum-road bridge, fatigue stress analysis, Model Code

1 Introduction

As a local structural component, the bridge deck supports vehicular live load directly before transmitting it to the main load-bearing girders. Repetitive wheel loadings can be as many as 10^7 cycles during the deck's service life [1]. Under repetitive loading, the material or components could fail prematurely at a load smaller than its capacity, called fatigue [2]. Several severe deck failures have raised concerns regarding concrete deck fatigue safety. In China, an approach bridge collapsed under the action of overloaded vehicles due to delayed retrofit work for fatigue cracks at the deck wet joint [3]. An existing highway deck of rail-cum-road bridge in China also suffered such defects as longitudinal and transverse cracks penetrated the top surface of the bridge deck, exacerbating the steel exposure at the bottom [4]. Fatigue damage is more prominent with high traffic demand and deck failure is generally triggered by overloaded vehicles. Issues regarding fatigue safety is not just present in China, but occurs in other countries as well. For example, the Throgs Neck Bridge in the USA exhibited evident cracks as short as ten years after opening to traffic due to tensile fatigue stress in the deck concrete, corrosion of reinforcement caused by deicing salt, wearing of the protective layer, and insufficient reinforcement [1]. In addition to threatening structural safety and traffic passage, bridge repair or replacement leads to economic and ecological loss.

As a result of such field observations of fatigue damage, the concept of a composite bridge deck that combines deck concrete with a steel plate on the bottom was proposed, offering increased load-bearing capacity and improved durability [5]. Since shear studs are known for shear slip failure on the interface between steel and concrete [6], perforated steel plate shear connectors (PBL) [7,8] or a combination of these two types of shear connectors [9] are used more and more often in composite decks.

Since the 1980s, researchers around the world have

Article history: Received Jan 14, 2022; Accepted Apr 14, 2022

conducted experiments on composite deck slabs and gained a tremendous amount of knowledge. Yang et al. [10] carried out constant-amplitude fatigue tests on simply-supported composite bridge decks under 4-point loading. The results show that the arrangement of PBL connectors does not have a significant impact on the performance of composite bridge decks. The fatigue failure mode of the composite bridge deck is, in most cases, bending failure caused by fatigue fractures of the bottom steel plate, regardless of whether the bottom steel plate is flat [10,11], profiled [9,12], or an orthotropic steel bridge deck [7,13–16]. However, Xu [17] pointed out that the longitudinal shear failure of deck concrete may occur if the perforated steel plates are not properly arranged. The composite decks are abundant in structural configurations and have excellent flexural fatigue resistance. Higgins and Mitchell [18] found that the stiffness of the composite deck under fatigue loading remains virtually unchanged compared to the static test. The fatigue problems associated with an orthotropic steel plate deck and pavement are essentially nonexistent in the case of a composite deck [15,16]. However, most of the above studies investigated the fatigue behavior of composite decks under positive bending moment and the simply-supported boundary condition is different from reality. It is also impossible to accurately determine the shear capacity of a composite deck by turning a simply-supported specimen upside down and simulating a negative bending moment with downward force [17].

In addition to experimental investigation, various approaches are available to evaluate the fatigue resistance of bridge decks. There are three main types of fatigue evaluation methods, specifically: the S-N curve method, fracture mechanics method, and method based on damage mechanics [19,20]. The latter two are more sophisticated, though the S-N curve method is still the dominant method practiced in engineering and adopted in various international codes. While standard fatigue truck is specified and fatigue provisions are available for orthotropic steel decks, no fatigue provision is available for highway concrete decks in the Chinese JTG 3362 Concrete Bridges Design Specifications.

PBL composite decks have been applied in steel plate girder bridges, steel box girder bridges, and truss bridges. The rail-cum-road truss bridge is regaining popularity due to its reduced land use and economic cost [21]. While studies on PBL composite bridge decks are available, research on the fatigue performance of such decks in rail-cum-road truss bridges remains scarce.

Fatigue safety is a concern when designing bridges, especially for innovative decks where similar successful applications are not yet available. As a case study, a novel type of PBL composite bridge deck supported on closely-spaced crossbeams in the newly-built Nansha Port Bridge in China is investigated. This paper adopts a cost-effective approach for the preliminary evaluation of the fatigue performance of the composite bridge deck. The fatigue assessment adopts code methods founded on the S-N curve and Miner's rule of linear accumulation of fatigue damage for fatigue resistance. For the fatigue load effect, we used the standard fatigue truck provided in Chinese JTG D60 General Specifications and traffic flow gathered from a nearby site for a more realistic simulation. The fatigue life associated with bending failure, shear failure, and concrete cracking were calculated and the dominant failure mode was identified. Analysis results show that the fatigue performance of this particular bridge deck is satisfactory under design conditions. However, further exploration is necessary considering the possibility of overloading and understrength.

2 Case study bridge

The newly constructed Nansha Port Bridge has a central span of 175 m, the largest among rail-cum-road continuous parallel-chord truss bridges in China. The bridge consists of 30 panels, with an internode length of 12.5 m for the main span and 12.75 m for the side span, as shown in Fig. 1(a). Figure 1(b) shows the bridge's cross-section, where the center-to-center distance of the two main trusses is 15.0 m. A two-direction six-lane highway deck with a width of 34.2 m is located at the top of the truss bridge. Figure 1(b) also shows the arrangement of traffic lanes. The distance between the centerline of Lanes 1, 2, and 3 and the bridge centerline is 3.625, 7.375, and 11.125 m, respectively.

Densely distributed crossbeams and multiple stringers support the highway bridge deck, while shear studs on all crossbeams and the side trusses connect the deck with the bridge. Figure 2(a) shows the beam layout for half of the central span deck panels, where longitudinally, four evenly distributed crossbeams support each truss panel. Bridge deck load is transferred from the longitudinal beam and cross member to the main truss. This type of deck-supporting system transmits the bridge deck load longitudinally in the direction of the shorter panel span [22].

The bridge deck is a steel-concrete composite slab with PBL connectors, as shown in Fig. 2(b). Perforated rib strips (10 mm thick and 130 mm high) are placed in the longitudinal direction of the bridge, spaced 250 mm from center to center. With holes of 60 mm in diameter and 150 mm in spacing, transverse reinforcing steels are provided through the openings in the strips. It should be noted that no prestress strands are provided in the deck. Any possible longitudinal tensile stress has been adequately taken care of in the design stage by specifying the appropriate casting sequence of deck concrete.

The design strength of deck concrete is C60 (with a

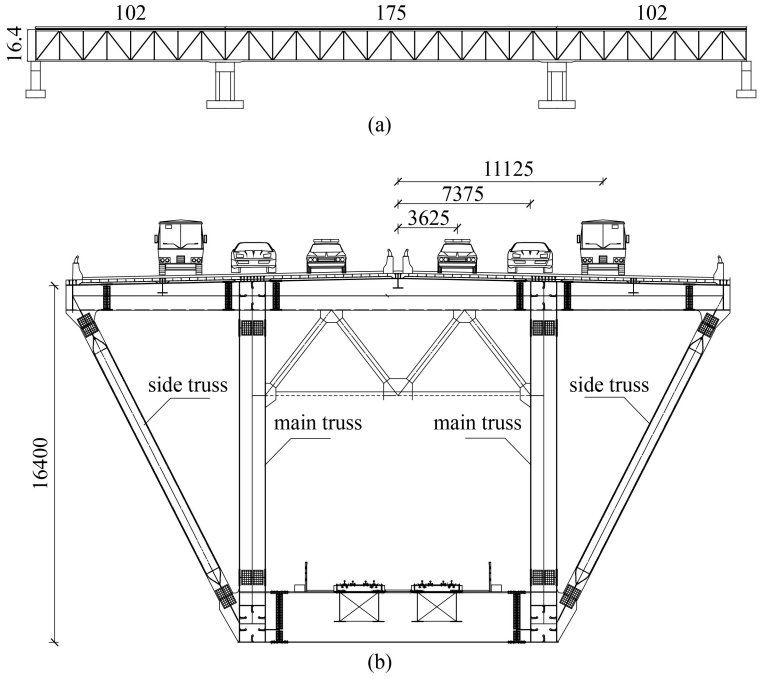

Fig. 1 The Nansha Port Bridge: (a) elevation of the bridge spans (m); (b) cross-section of the bridge structure, showing lane arrangement (mm).

95% probability of cubic compressive strength greater than 60 MPa) and the main structural components are made from Q420qE steel (yield strength of 420 MPa). Table 1 provides the primary geometry of the composite slab and deck reinforcement.

3 Fatigue stress analysis

3.1 Representative locations for analysis

In a rail-cum-road steel truss bridge, the bridge deck deflects under the repetitive action of vehicular wheel loading, but deck deformation is restrained at their connections with supporting members. It is foreseeable that the deck plate adjacent to supporting members is susceptible to fatigue damage. The main truss (with a height of 16.4 m) offers much larger stiffness and restraint for the deck plate (with a depth of 0.2 m) compared to crossbeams and stingers. Therefore, a significant transverse negative bending moment occurs where bending stiffness increases abruptly around the main truss. Restrained concrete shrinkage or temperature deformation will also cause additional transverse tensile stress on the deck near the main truss. Therefore, the new PBL composite deck is prone to longitudinal fatigue cracking at the edge of the main truss, as shown in Fig. 3(a) [23].

Since the bridge deck can be viewed as a continuous plate elastically supported on surrounding crossbeams and stringers/trusses, deck panels respond mainly to loads applied within several nearby panels. It is reasonable to treat the deck panel as a locally-loaded component and an arbitrary longitudinal panel can be a subject of investigation. For convenience, we selected a portion of the central span (shown as the blue rectangular box in Fig. 2(a)). The positions for the red rectangular box in Fig. 2(a) are herein identified as “areas of concern” or hotspots in Figs. 3(b) and 3(c).

3.2 Finite element model

A hybrid finite element model was constructed using ABAQUS software to facilitate an understanding of stress distribution in the composite bridge deck. The model consists of the entire bridge structure, as shown in Fig. 4.

While most steel truss members are modeled with beam element B31, shell element S4R is adopted for modeling upper chords of the main truss and tied to connecting beam elements. The model uses continuous solid element C3D8R for deck concrete and T3D2 for reinforcing steel embedded in the concrete. As linear elastic analysis is performed for fatigue stress evaluation, shear studs and PBL connectors are simulated as TIE connections where no slip is assumed to occur. Although PBL connectors offer excellent stiffness even after millions of loading cycles [18], one must bear in mind that this assumption is a mere approximation aiming for simplicity and efficiency in modeling. The composite deck model employs a varying density of mesh refinement. The mesh size in the three truss panels (roughly 40 m) in the midspan region is 0.1 m, gradually increasing to 0.75 m throughout the rest of the model, as shown in Fig. 4.

The accuracy of the finite element model has been

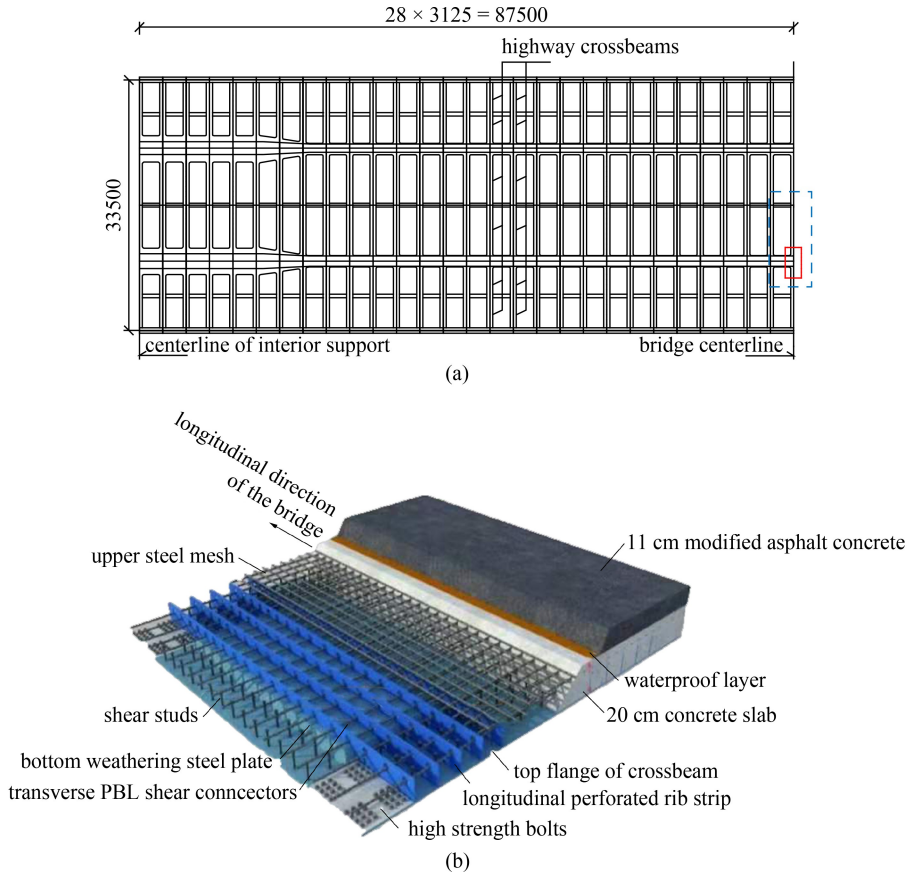

Fig. 2 Highway deck of the Nansha Port Bridge: (a) supporting beam layout of the deck (mm), showing half of the central span with crossbeams and stringers; (b) structural diagram of the composite deck, showing weathering steel plate, perforated rib strips, shear studs, and reinforcement.

Table 1 Main properties of the deck in the Nansha Port Bridge

dimension	value
deck thickness	200 mm
haunch height	50 mm
concrete cover	30 mm
weathering steel plate thickness	10 mm
perforated rib strips (thickness−height−spacing)	10 mm–130 mm–250 mm
PBL shear connectors (hole diameter−spacing−reinforcement)	Φ60 mm–150 mm–φ8 mm
longitudinal reinforcement	φ8 mm–250 mm
effective depth, longitudinal	170 mm
transverse reinforcement	φ8 mm–200 mm
effective depth, transverse	162 mm

verified by comparing analysis results with field measurements of the bridge deck. For illustration, Fig. 5 only shows a comparison between the measured stress and finite element results under one loading case of an in-situ bridge load test. In this loading case, a 49 t double-axle construction truck (with a rear axle weight of 40 t and front-rear axle spacing of 3.78 m) was driving at 10 km/h across the bridge and the loading lane was 3.5 m from the bridge centerline. The measuring points 1, 2, and 3 shown in Figs. 5(a)–5(c) are installed at positions 1, 3, and 4 of the midspan deck panel, respectively (see Fig. 3(c)). The field measurements were obtained by multiplying the measured strain by the modulus of elasticity, which is 36000 MPa for C60. The construction truck was represented by surface pressure during finite element simulation and the same method will be used for the standard fatigue truck modeling, which is explained in detail in Subsections 3.3 and 3.4.

From Fig. 5, we can see that the stress history from finite element simulation is in good agreement with the measured values. The maximum tensile stress in concrete occurs at position 1 of the bridge deck, making it feasible to categorize the areas near the main truss as hotspots of fatigue cracking. As the truck passes slowly on the bridge, each axle causes a stress cycle at the hotspot, with the maximum stress caused by the rear axle, which is approximately four times higher than that by the front axle. The maximum transverse tensile stress (0.92 MPa) at the main truss from the finite element simulation is 24.3% larger than the measured value (0.74 MPa). The connection between the truss member and the deck concrete in the finite element model is fully rigid, resulting in a more significant analytical value. Overall,

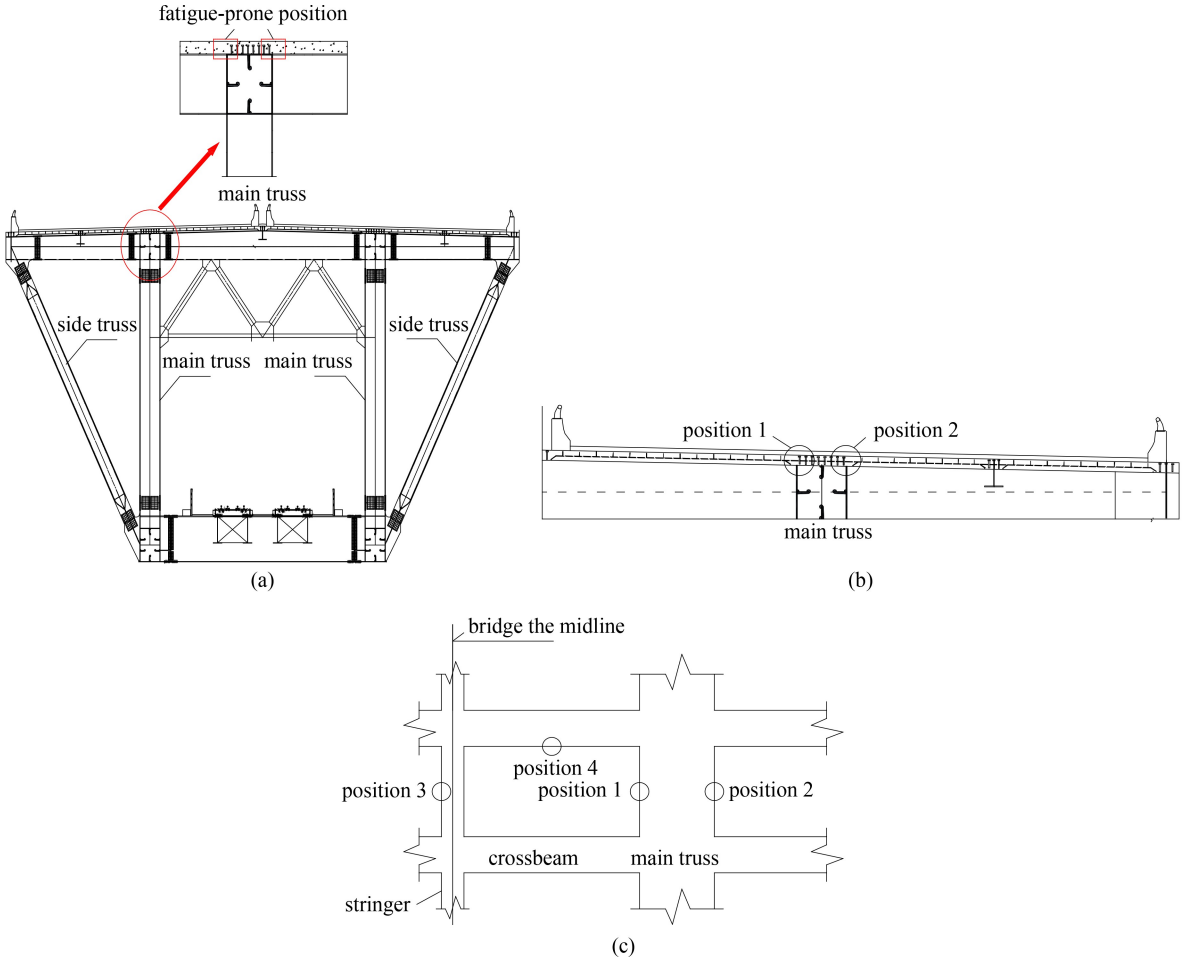

Fig. 3 Schematic view of fatigue-prone positions in composite deck of the Nansha Port Bridge: (a) elevation view; (b) elevation view in close-up; (c) plan view.

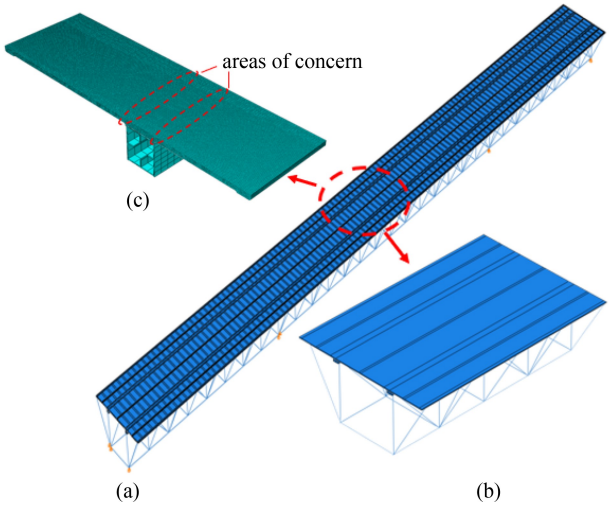

Fig. 4 Finite element model of the Nansha Port Bridge: (a) overview of the entire truss bridge, showing highway deck, truss members, and boundary condition; (b) enlarged view of the central portion of the bridge; (c) enlarged view of the bridge deck near the main truss, showing upper chord truss member and areas of concern (hotspots) in the deck.

the finite element analysis simulates the stress characteristics of the bridge deck under vehicle loading reasonably well.

3.3 Most unfavorable transverse loading position

According to China's highway bridge design code [24], fatigue load model III should be used for fatigue analysis of bridge decks. The standard fatigue vehicle has four axles, each weighing 120 kN. With transverse wheel spacing of 2 m, the wheel footprint is 0.4 m × 0.8 m considering the thickness of the pavement layer. This paper mainly focuses on the fatigue failure risk of the composite bridge deck from transverse negative bending moment under the repeated action of vehicle load. When the vehicle runs in different transverse positions of the bridge deck, the stress state of the bridge deck differs. To determine the most unfavorable transverse loading position for the hotspot near the main truss, we loaded two 60 kN wheel loads (simulated as surface pressure) along the midspan cross-section of the central span at a spacing of 0.1 m. Figure 6 shows the transverse tensile stress at hotspots 1 and 2 of the bridge panel for various

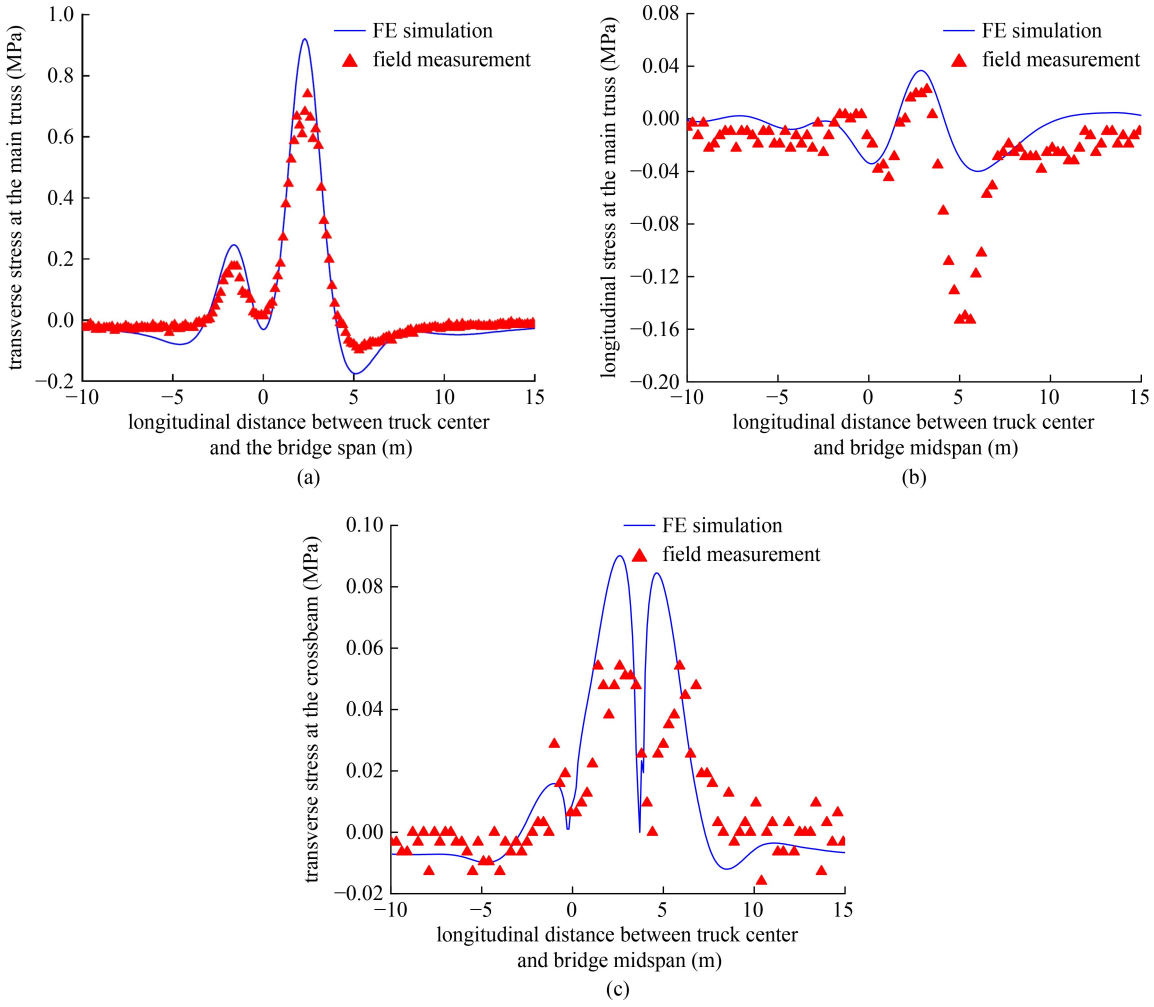

Fig. 5 Comparison between finite element simulation and experimental results: (a) transverse stress at measuring point 1; (b) longitudinal stress at measuring point 2; (c) transverse stress at measuring point 3.

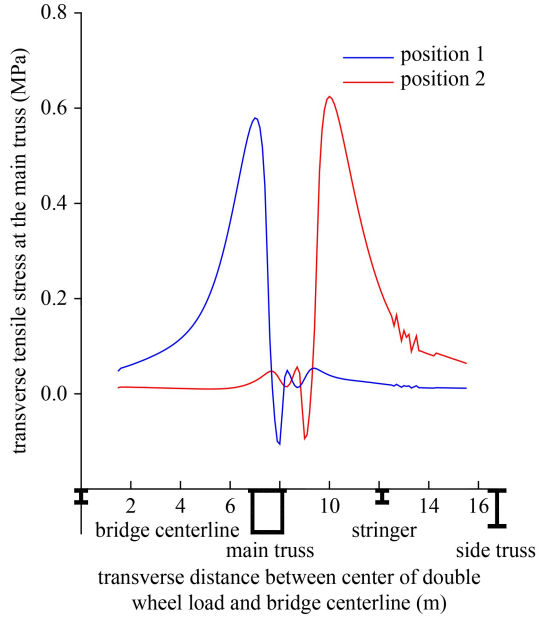

Fig. 6 Variation of transverse stress at the main truss with varying wheel positions.

positions of a standard fatigue truck.

According to Fig. 6, when the transverse distance between the truck center and the centerline of the bridge is 7 m, the tensile stress at Position 1 of the deck panel near the main truss reaches its maximum. We shall denote this position as Lane 4. The transverse location of the truck center corresponding to the maximum tensile stress at position 2 of the main truss bridge panel is 10 m from the bridge centerline, denoted as Lane 5. Considering that most vehicles drive along the lanes in practice, we shall load the standard fatigue truck longitudinally in the unfavorable lane positions mentioned above and the design Lanes 1, 2, and 3 afterwards, as shown in Fig. 1(b).

3.4 Stress history from longitudinal loading

The fatigue truck is then longitudinally loaded along the centerlines of Lanes 1, 2, 3, 4, and 5 by the DLOAD subroutine of ABAQUS. The fatigue vehicle is modeled as eight uniform surface pressure loads according to the standard fatigue vehicle's wheel footprint sizes and axle load. Figures 7 and 8 show the transverse tensile stress

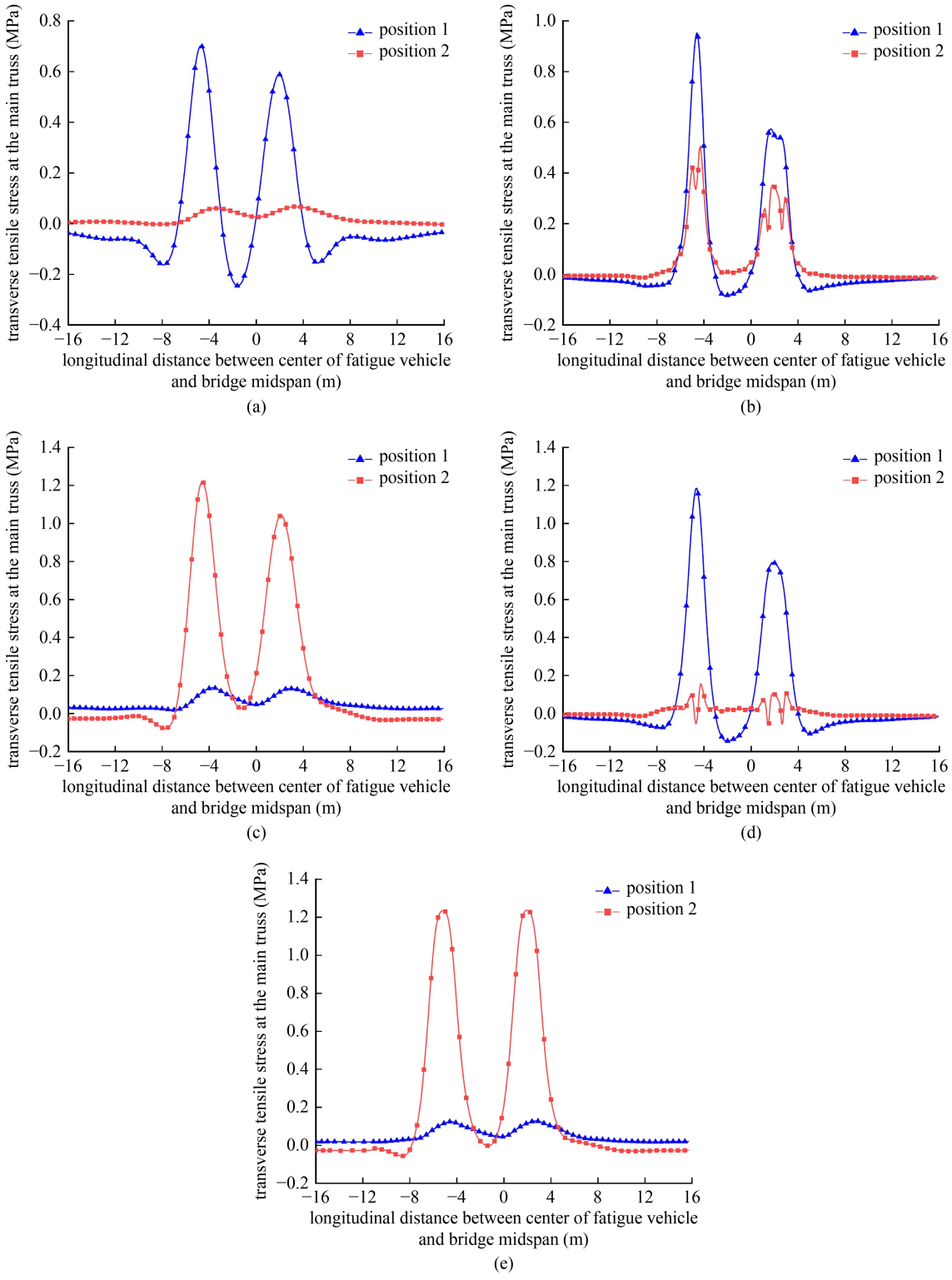

Fig. 7 Transverse tensile stress history of deck concrete under standard fatigue truck loading: (a) Lane 1; (b) Lane 2; (c) Lane 3; (d) Lane 4; (e) Lane 5.

and transverse compressive stress of the bridge panel at the areas of concern, respectively, for each fatigue vehicle loaded lane.

As shown in Figs. 7 and 8, since the bridge deck is a locally-stressed component with a short influence line, the vehicle will produce significant stress on the hotspot only when its wheels run close to the position. Therefore, each of the front and rear axles of the fatigue vehicle will cause peak stress when passing through the area of concern.

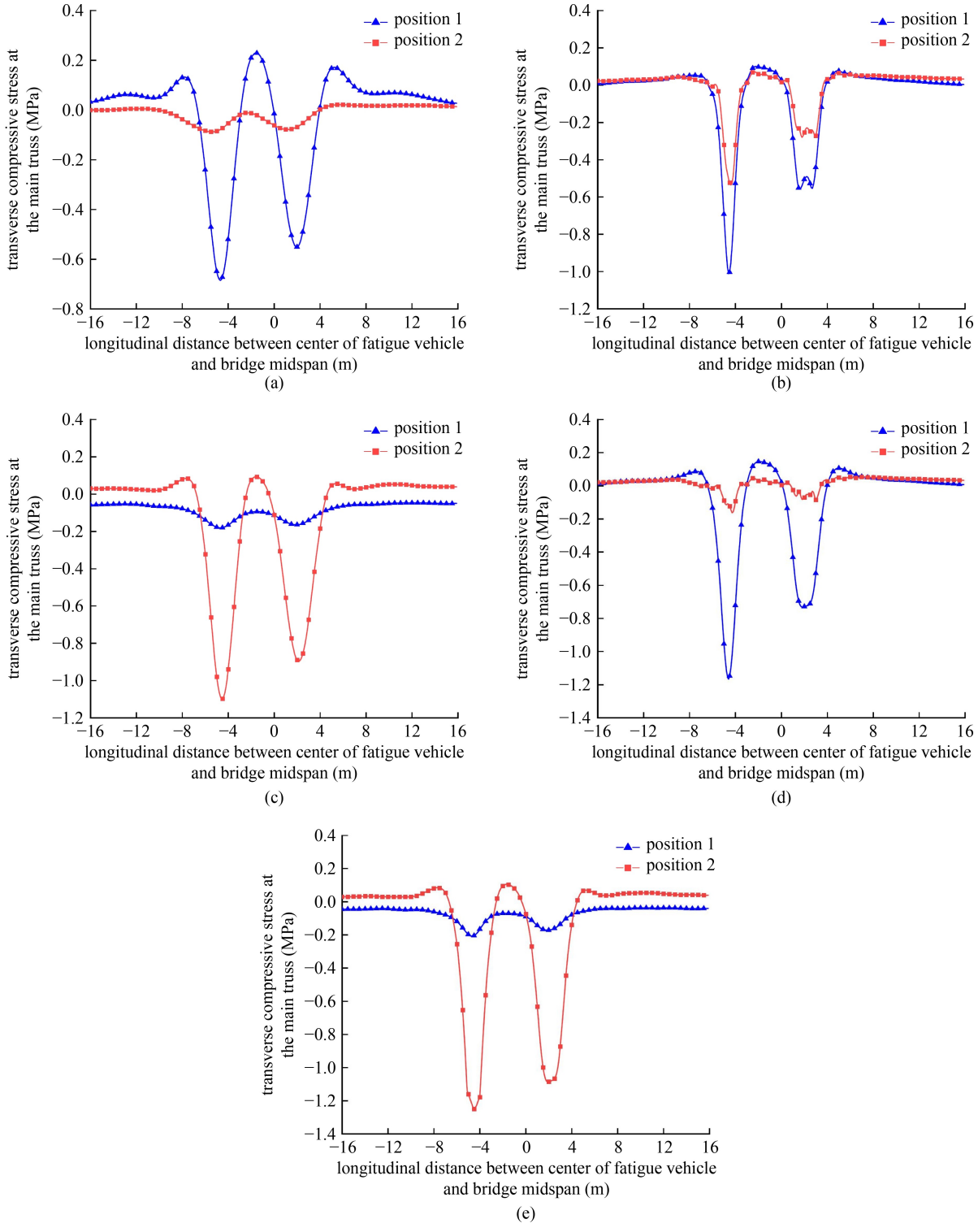

Fig. 8 Transverse compressive stress history of deck concrete under standard fatigue truck loading: (a) Lane 1; (b) Lane 2; (c) Lane 3; (d) Lane 4; (e) Lane 5.

For position 1, the stress response caused by the fatigue truck running in Lane 4 is the most significant. For position 2, the fatigue vehicle running in Lane 5 produces the maximum stress response. When the vehicle center is 4 m away from the midspan for Lane 4 loading, the tensile stress on the top surface of the bridge deck, at 1.625 m from the midspan, reaches the maximum of 1.185 MPa.

The deck concrete's stress contour under Lane 4 loading from finite element analysis is shown in Fig. 9, where stress in the transverse direction (1.185 MPa) is higher than the longitudinal stress (0.120 MPa). It can be

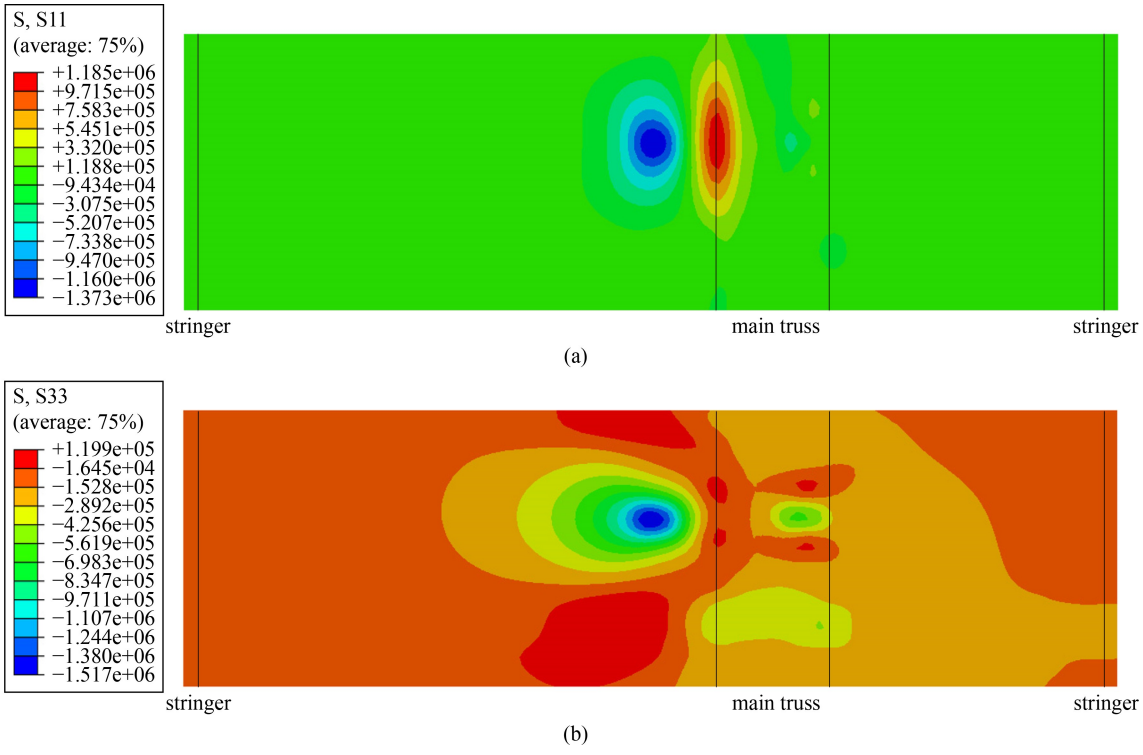

Fig. 9 Stress contour at areas of concern: (a) transverse stress; (b) longitudinal stress.

seen that the bridge deck in the transverse negative bending moment region is susceptible to fatigue failure.

3.5 Summary of fatigue stress of bridge deck

In addition to the stress caused by a standard fatigue truck, the stress state of the bridge deck concrete near the main truss could also be affected by other load effects, such as self-weight, shrinkage, and gradient temperature. Since the deck concrete was cast in situ where steel trusses support the deck's self-weight and the stress caused by pavement is only about 0.1 MPa, the effect of self-weight is insignificant, thus neglectable in the fatigue evaluation.

However, initial tensile stress does exist in the deck concrete before the bridge operation because the stiffness of the main truss restrains the free shrinkage deformation. Due to the significant stiffness of the main truss and the strong constraint, the initial transverse tensile stress caused by restrained concrete shrinkage near the main truss can reach 0.4 MPa. The calculation shows that the secondary stress caused by concrete shrinkage increases with age [23], as shown in Fig. 10.

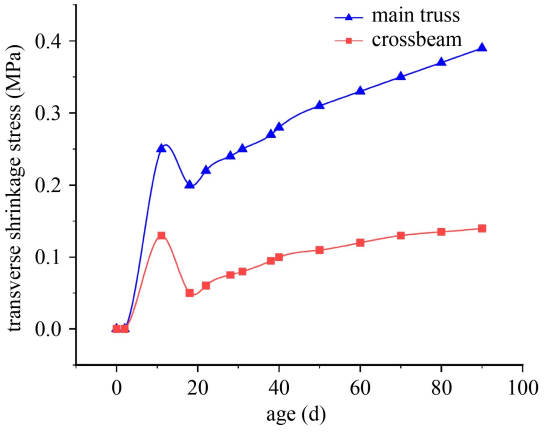

Fig. 10 Transverse shrinkage stress developed in bridge deck.

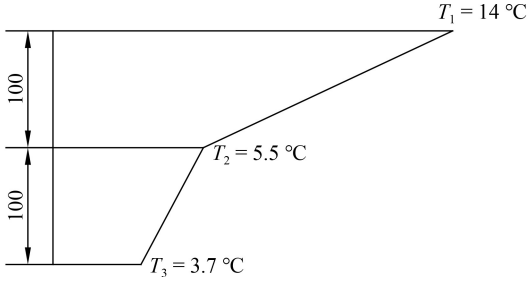

Fig. 11 Schematic diagram of positive vertical temperature gradient in bridge deck (mm).

The stress caused by gradient temperature during bridge operation should not be neglected. According to the specification [24], Fig. 11 shows the composite deck's vertical positive temperature gradient distribution. When calculating the negative gradient temperature, the temperature difference is multiplied by –0.5. Under negative gradient temperature, the transverse tensile stress on the top surface at positions 1 and 2 are 1.330 and 1.180 MPa, respectively, while the bottom compressive

stresses are 0.175 and 0.162 MPa, respectively. Under positive gradient temperature, the transverse compressive stresses on the top surface at positions 1 and 2 are 1.979 and 1.853 MPa, respectively, while the tensile stresses on the bottom surface are 0.721 and 0.718 MPa, respectively.

3.5.1 Before concrete cracking

The initial tensile stress caused by shrinkage and gradient temperature will directly change the value of the stress history of the areas of concern. Position 1 is where the most unfavorable stress in the bridge deck occurs. Considering the shrinkage and gradient temperature stress during bridge operation, the maximum tensile stress on the top surface is $\sigma_{max} = 1.185 + 0.4 + 1.33 = 2.915$ MPa and the minimum stress is $\sigma_{min} = -0.01 + 0.4 - 1.589 = -1.979$ MPa. Accordingly, the maximum compressive stress on the bottom surface is $\sigma_{max} = -1.26 + 0.4 - 0.175 = -1.035$ MPa and $\sigma_{min} = 0.22 + 0.4 + 0.721 = 1.341$ MPa. In the above expression, a positive value stands for tensile stress, while a negative value means compressive stress. Therefore, deck concrete is in a tension-compression fatigue stress state during bridge service, which is highly unfavorable for fatigue performance. Table 2 summarizes the fatigue stress and parameters at position 1 for the following fatigue evaluation.

3.5.2 After concrete cracking

Once concrete cracks, it is usually neglected for tensile resistance. Since stress redistribution occurs inside the structure after concrete cracking, the additional tensile stress is redistributed onto the reinforcing steel. Reinforced concrete flexural members can typically carry loads until the fatigue fracture of reinforcement.

Therefore, the stress calculation adopts the cracked section since concrete is neglected after tensile failure and reinforcing steel is assumed to accept all tensile force. Based on section properties of the cracked section and the ratio of elastic modulus between steel and concrete, we first calculated the tensile stresses in reinforcement under maximum and minimum bending moments, after which obtained the fatigue stress range after concrete cracking. If we consider the long-term modulus of elasticity of concrete under fatigue loading as 1.7×10^4 MPa, the estimated maximum stress range $\Delta\sigma_{Rsk}$ is 40.6 MPa. Figure 12 shows the stress history of tensile reinforcing steel under the most critical loading condition of Lane 4.

4 Fatigue assessment of the composite deck

The fatigue performance of the new PBL composite deck supported by densely spaced crossbeams remains unclear. Since no fatigue provision for concrete members is available in current highway bridge design specifications in China, this section follows the main-stream standard, fib Model Code for Concrete Structures 2010 proposed by the International Federation of Structural Concrete [25], for a preliminary assessment of fatigue performance of the bridge deck. Although relevant code provisions are derived from research on reinforced concrete slabs, it is assumed that these provisions are also applicable to composite decks with PBL and flat steel plates.

4.1 Code provision for fatigue resistance

Fatigue is considered one of the ultimate limit states for which the consequence of failure is not severe. CEB fib Model Code is widely used and has extensive treatment on fatigue design or evaluation of concrete structures. The specification defines four levels of fatigue evaluation methods with increasing refinement: Level I for qualitative analysis, Level II and III based on constant amplitude loading (II for infinite life; III for finite life), and Level IV for variable amplitude loading and Palgram-Miner rule. It is usually necessary to check both flexural and shear fatigue capacity.

A Level I analysis determined that the primary concern is flexural fatigue performance in negative transverse

Table 2 Fatigue stress and parameters at position 1

stage	stress or parameter	value (MPa)
before concrete cracking	concrete stress at the main truss (top surface) under the action of fatigue truck	1.185
	concrete stress at the main truss (bottom surface) under the action of fatigue truck	–1.260
	concrete stress at the main truss (top surface) under the negative temperature gradient	1.330
	concrete stress at the main truss (bottom surface) under the positive temperature gradient	–0.175
	secondary stress due to restrained concrete shrinkage	0.400
	concrete's modulus of elasticity	36000
after concrete cracking	stress range of reinforcement at the main truss	40.6
	concrete's modulus of elasticity (considering fatigue deformation)	17000

Note: In this table, tensile stress is positive and compressive stress is negative.

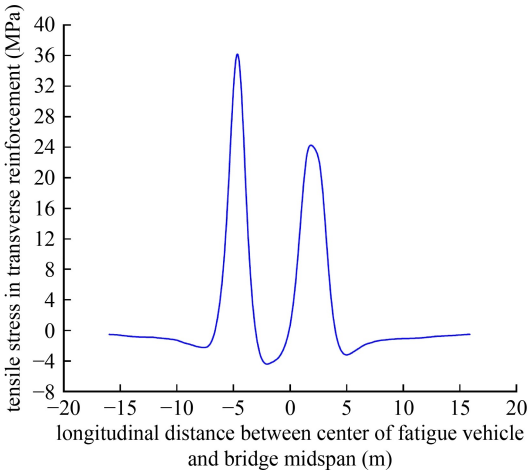

Fig. 12 Transverse tensile stress history of reinforcing steel under standard fatigue truck loading of Lane 4.

bending. Since the bottom steel plate and PBL have enhanced bending rigidity and flexural fatigue capacity for the deck plate under positive bending moment, it would not control the deck's fatigue performance. While there could be alternating tensile stress near interior supports in the longitudinal direction, adjusting the concrete casting sequence would adequately address the issue. Therefore, this paper focuses on the flexural fatigue performance of the composite bridge deck under a transverse negative bending moment. In contrast to reinforced concrete slabs without the shear stirrups that shear fatigue failure usually governs, shear fatigue in composite bridge decks should not be a significant concern as there are perforated steel plates. Nevertheless, shear fatigue will also be checked for completeness. We also include a fatigue cracking analysis of concrete because the propagation of cracks under negative bending moment will lead to steel corrosion and concrete carbonization, which can influence the durability of the bridge deck.

Afterwards, a Level III fatigue analysis will be performed. According to the fib Model Code for Concrete Structures 2010 [25], the fatigue design of bridge decks includes the flexural, direct shear, and punching shear fatigue modes. As explained, both flexural and shear fatigue strength should be checked. In flexural check, both stress range in steel and maximum compressive stress in concrete are the controlling variables, while cracking assessment depends on concrete tensile stress. We will also evaluate shear fatigue in one-way beam shear and two-way punching shear.

4.2 Bending fatigue

Figure 12 shows the stress history of reinforcement at hotspot 1 of the composite bridge deck under the action of Lane 4. The maximum tensile stress range of the steel is $\Delta\sigma_{\mathrm{Rsk}} = 40.6$ MPa. Substituting this into the S-N curve for reinforcing steel, or Eq. (1), the calculated fatigue life of the steel is 9.33×10^7 cycles.

$$\begin{cases} \log \Delta\sigma_{\mathrm{Rsk}} = 4.12 - 0.33 \log N, & N \leqslant 10^7, \\ \log \Delta\sigma_{\mathrm{Rsk}} = 3.202 - 0.2 \log N, & N > 10^7. \end{cases} \tag{1}$$

When maximum compressive stress satisfies $\gamma_{\mathrm{Ed}}\gamma_{\mathrm{c,fat}}\sigma_{\mathrm{c,max}} \leqslant 0.45 f_{\mathrm{cd,fat}}$ for concrete in compression, the concrete will not fail under fatigue. The partial load factor, γ_{Ed}, is 1.0 and the partial safety factor for concrete under fatigue loading, $\gamma_{\mathrm{c,fat}}$, is 1.5. According to the specification, the fatigue strength of concrete, $f_{\mathrm{cd,fat}}$, is calculated as 34.68 MPa. After concrete cracks, fatigue stress in the compressive zone is 2.48 MPa. Since $1 \times 1.5 \times 2.48 = 3.72$ MPa $< 0.45 \times 34.68 = 15.6$ MPa, the fatigue requirement for concrete in compression is met.

4.3 Direct shear fatigue

The shear fatigue life of the composite deck can be evaluated according to Eq. (2),

$$\log N = 10(1 - V_{\max}/V_{\mathrm{Re}}), \tag{2}$$

where $V_{\max}$ stands for the maximum shear force and V_{Re} is the shear capacity of the deck. The fatigue life corresponding to both transverse and longitudinal shear failure is calculated. The control section for shear calculation is at a distance of effective plate thickness away from the edge of support, which is 170 mm from the edge of support for the Nansha Port Bridge.

4.3.1 Shear fatigue in the transverse direction

Longitudinal perforated steel plates, similar to stirrups, are present inside the reinforced concrete members of the deck. Together, the perforated steel plate and concrete provide the shear capacity of the composite deck [26], i.e., $V_{\mathrm{Re}} = V_{\mathrm{Re,c}} + V_{\mathrm{Re,s}}$. The shear capacity attributed to concrete, $V_{\mathrm{Re,c}}$, is calculated according to Eqs. (3) and (4),

$$V_{\mathrm{Re,c}} = k_{\mathrm{v}} \frac{\sqrt{f_{\mathrm{ck}}}}{\gamma_{\mathrm{c}}} z b_{\mathrm{w}}, \tag{3}$$

$$k_{\mathrm{v}} = \frac{180}{1000 + 1.25z}, \tag{4}$$

where the partial safety factor for concrete, γ_{c}, is 1.5, and the shear design factor, k_{v}, is calculated according to Eq. (4). The effective shear depth, z, is 170 mm and the concrete compressive strength, f_{ck}, is 60 MPa. The width of the control section, b_{w}, is determined by extending the load edge 45° towards the control section, that is, $b_{\mathrm{w}} = 0.4 + 2 \times 1.04 = 2.48$ m. According to Eq. (3), the shear capacity of the deck provided by concrete, $V_{\mathrm{Re,c}}$, is 325 kN.

The perforated steel plate functions similarly to stirrups and its shear capacity can be calculated according to Eq. (5),

$$V_{\mathrm{Rd,s}} = \frac{A_{\mathrm{sw}}}{s_{\mathrm{w}}} z f_{\mathrm{ywd}} \cot\theta, \tag{5}$$

where the design strength of steel plate for shear reinforcement, f_{ywd}, is 275 MPa; the spacing between the perforated plates, s_{w}, is 350 mm; the height of the perforated steel plate, z, is 120 mm. The net area of the perforated steel plate on the control section, A_{sw} is taken as $(2480 - 17 \times 60) \times 8 = 11680$ mm^2. The angle between the inclined shear failure surface and the horizontal line, θ, could be 30 degrees for a reinforced concrete structure [26]. The calculated shear capacity provided by the perforated steel plate is 1905 kN.

The transverse shear capacity of the composite deck is thus $V_{\mathrm{Re}} = V_{\mathrm{Re,c}} + V_{\mathrm{Re,s}} = 2230$ kN. The maximum vertical shear force at the control section is 46.4 kN when a standard fatigue vehicle is loaded in the most critical position. According to Eq. (2), the transverse direct shear fatigue life of the composite deck is calculated as 6.16×10^9 cycles.

4.3.2 Shear fatigue in the longitudinal direction

Similarly, the longitudinal shear fatigue performance in the longitudinal direction is evaluated for the control section 170 mm away from the crossbeam support.

The width of the control section, b_{w}, equals $0.8 + 2 \times 0.8 = 2.4$ m and the deck's shear capacity provided by concrete, $V_{\mathrm{Re,c}}$, is 314 kN. As the perforated steel plates are arranged along the longitudinal direction, which functions similarly to a steel web, their shear capacity can be calculated using $V_{\mathrm{upbl}} = f_{\mathrm{vd}} A_{\mathrm{pbl}}$, where the design shear strength of the steel plate, f_{vd}, is 160 MPa. The net cross-sectional area of eight perforated plates, A_{pbl}, equals $(120 - 60) \times 8 \times 8 = 3840$ mm^2. Therefore, the shear capacity provided by the perforated steel plate is $V_{\mathrm{us}} =$ 614 kN and the total longitudinal shear capacity in the longitudinal direction is 928 kN. Likewise, loading a fatigue vehicle in the most unfavorable position results in a maximum vertical shear force of 53 kN at the control section. According to Eq. (2), the composite deck's longitudinal direct shear fatigue life is 2.63×10^9 cycles.

4.4 Punching shear fatigue

The punching shear fatigue performance of the composite deck is also evaluated according to Eq. (2), where the control section for punching shear failure is located 0.5 times the effective depth from the wheel edge. The punching shear capacity attributed to concrete is calculated from Eqs. (6)–(8):

$$V_{\mathrm{Rd,c}} = k_{\psi} \frac{\sqrt{f_{\mathrm{ck}}}}{\gamma_{\mathrm{c}}} b_0 d_{\mathrm{v}}, \tag{6}$$

$$k_{\psi} = \frac{1}{1.5 + 0.9 k_{\mathrm{dg}} \psi d} \leqslant 0.6, \tag{7}$$

$$\psi = 1.5 \frac{r_{\mathrm{s}}}{d_{\mathrm{v}}} \frac{f_{\mathrm{y}}}{E_{\mathrm{s}}}. \tag{8}$$

The punching shear capacity attributed to steel is calculated according to Eq. (9),

$$V_{\mathrm{Rd,int}} = \sum A_{\mathrm{S}} f_{\mathrm{yd}} (f_{\mathrm{t}}/f_{\mathrm{y}})_{\mathrm{k}} \sin\alpha_{\mathrm{ult}}, \tag{9}$$

where d_{v} denotes the effective depth of the bridge deck; k_{dg} is the coefficient related to concrete's coarse aggregate, taken as 1.0; r_{s} is the longer distance between support and inflection point in transverse and longitudinal directions, which is 1430 mm for the case study bridge (approximately 0.22 times the span length of the deck panel); ψ stands for the angle of rotation at the supports; the effective depth against bending, d, is 170 mm; the area of steel reinforcement, A_{s}, is 2289.1 mm^2; the design tensile strength of reinforcing steel, f_{yd}, is 330 MPa; $(f_{\mathrm{t}}/f_{\mathrm{y}})_{\mathrm{k}}$ stands for the ratio of tensile strength to yield strength of the steel, taken as 1.43; the angle between the reinforcement and the inclined failure surface, α_{ult}, is taken as 25° according to the specification.

From Eqs. (6) and (9), $V_{\mathrm{Rd,c}} = 490$ kN and $V_{\mathrm{Rd,int}} =$ 456 kN, thus the punching shear capacity of the bridge deck is 946 kN. According to Eq. (2), the punching shear fatigue life of the composite deck under one wheel load of 60 kN is 2.29×10^9 cycles.

4.5 Concrete cracking

The cracking of concrete can be evaluated according to its tensile fatigue stress. For deck concrete near the main truss, the upper part of the section is in tension and the lower part in compression, with stress gradient distribution consistent with a flexural member. Therefore, the bending tensile strength is appropriate for representing the tensile strength of concrete.

Fatigue life evaluation of concrete is based on the cyclic maximum and minimum stresses (σ_1, σ_2). When there are stress reversals of tension and compression and $\sigma_1 > 0.026 |\sigma_{\mathrm{c,max}}|$, the fatigue life of concrete can be computed according to Eq. (10),

$$\log N = 12(1 - S_{\mathrm{td,max}}), \tag{10}$$

in which: $S_{\mathrm{td,max}} = \gamma_{\mathrm{Ed}} \times \sigma_{\mathrm{ct,max}} / f_{\mathrm{ctd,min}}$; N is the fatigue life of concrete; the maximum compressive stress of concrete, $\sigma_{\mathrm{c,max}}$, is 1.589 MPa; $S_{\mathrm{td,max}}$ denotes the maximum tensile stress level; the partial load factor under fatigue loading,

γ_{Ed}, is 1.0; the maximum tensile stress, $\sigma_{ct,max}$, is 2.915 MPa; $f_{ctd,min}$ stands for the bending tensile strength, which is 6.2 MPa for C60 concrete [27].

According to Eq. (10), the tensile fatigue life of concrete at hotspot 1 is 2.28×10^6 cycles. Therefore, concrete is very likely to suffer tension fatigue cracking during the service life of the Nansha Port Bridge, which is detrimental to its durability.

5 Discussion

5.1 Dominant fatigue failure mode

Fatigue assessment provisions in fib Model Code 2010 [25] are relatively comprehensive and include four levels of assessment methods. The Level III fatigue assessment method can predict fatigue life and determine the controlling fatigue failure mode. The flexural fatigue life is determined from the compressive stress in concrete or the tensile stress in reinforcing steel. The shear fatigue life calculation considers both direct shear and punching shear of the deck. Moreover, the fatigue cracking life can be evaluated from the tensile stress in concrete. This paper calculates the load effect based on the standard fatigue truck in China, while fatigue resistance is calculated from the fib Model Code. Although this is the best practice available, it is possible that different standards have varying levels of reliability. Therefore, further research is required to accommodate this potential incompatibility and improve the fatigue design of China's highway concrete bridge specifications.

From Section 4, the fatigue life of the composite deck for bending failure, direct shear failure, and punching shear failure is 9.33×10^7, 2.63×10^9, 2.29×10^9, respectively. Comparing fatigue lives of the above three failure modes, the bridge deck would fail under bending fatigue in the negative moment region. Thus, the bending fatigue failure is the dominant fatigue failure mode of the composite bridge deck and its fatigue life is 9.33×10^7 stress cycles. Miner's linear damage criterion could be used to calculate fatigue damage, specifically, $D = \sum n_i/N_i$, where D = the number of cycles n/fatigue life N. Assuming the yearly traffic flow in Lane 4 is 1.5 million standard fatigue vehicles [28], the computed annual fatigue damage D is 0.018, meaning the deck will be damaged after 56 years of service due to fatigue fracture of steel reinforcement.

In addition, the maximum concrete stress at the deck top surface reaches 2.915 MPa near the main truss and its corresponding tensile fatigue life is 2.28×10^6 cycles. However, there is a difference between the number of stress cycles due to gradient temperature and truck loading. One stress cycle is produced per day for the thermal effect and we could assume 50% of the total cycles per year for both positive and negative gradient temperature. The number of stress cycles generated from fatigue live load actions is 1.5 million vehicles per year, which is then multiplied by two stress cycles per vehicle. According to Miner's linear damage criterion, the annual fatigue damage D is 0.181 under the superposition of temperature, shrinkage, and fatigue vehicle load. Concrete fatigue cracking is likely to occur on the top surface of the deck near the main truss shortly after six years of service. This type of premature longitudinal crack is primarily due to transverse tensile stress. Once the concrete cracks, the tensile stress in reinforcing steel increases significantly, leading to flexural fatigue failure of the bridge deck. Although the composite deck is designed to perform with cracks during most of its service life, these cracks may accelerate reinforcement corrosion and concrete deterioration, reducing the durability of the bridge deck. Therefore, one should give full consideration to concrete cracking in the deck design.

5.2 Effect of overloading

In China, vehicle overloading is a threat to bridge integrity. Therefore, according to the controlling fatigue failure mode discussed above, fatigue assessment of the composite deck under vehicle overloading is evaluated. Considering 20% overload, the fatigue life and cracking life when the proportion of overloaded vehicles to total traffic flow is 10%, 30%, and 50% are shown in Table 3.

Table 3 shows that the fatigue cracking life of the composite deck reaches one year when the proportion of overloaded vehicles is 50% and the deck fails after 35.4 years of service. We can see that overloading greatly influences the fatigue life and cracking life of the composite bridge deck and, especially, fatigue cracking.

5.3 Effect of understrength of materials

Randomness at the material level is constantly present for structural members. Although steel exhibits little variability, the variability in concrete strength is nevertheless unneglectable, which invariably affects the fatigue cracking of concrete. Therefore, if bending failure is considered as the dominant fatigue mode, it is necessary to assess fatigue of the composite deck under concrete understrength. The fatigue cracking life of the composite deck is shown in Table 4 when the percentage of concrete understrength is 5%, 10%, and 15%.

Table 4 shows that the fatigue cracking life of the composite deck reaches one year when the concrete's bending tensile strength is just 15% lower than the design value. Even though the total fatigue life of the bridge deck is not severely impaired, the understrength of concrete significantly affects the fatigue cracking of the composite bridge deck.

Table 3 Fatigue assessment of the composite deck under overloading

percentage of overloaded vehicles (%)	steel stress range $\Delta\sigma_{Rsk}$ (MPa)	fatigue life (year)	concrete stress level $S_{td,max}$	cracking life (year)
0	40.6	55.6	0.47	5.5
10	48.7	54.0	0.56	3.8
30	48.7	42.8	0.56	1.8
50	48.7	35.4	0.56	1.0

Table 4 Fatigue assessment of the composite deck for understrength of materials

percentage of understrength (%)	concrete strength $f_{ctd,min}$ (MPa)	concrete stress level $S_{td,max}$	cracking life (year)
0	6.20	0.47	5.5
5	5.89	0.49	4.4
10	5.58	0.52	2.0
15	5.27	0.55	1.0

6 Conclusions

The bridge deck is the structural component most vulnerable to fatigue damage due to repetitive vehicular loading. An innovative steel-concrete composite bridge deck system comprised of a flat steel plate and perforated plate (PBL) shear connectors supported on closely spaced crossbeams has been proposed for rail-cum-road bridge applications. Although promising and advantageous, its fatigue performance remains unclear, especially under the action of the hogging moment. To evaluate the fatigue performance of such a composite bridge deck, the Nansha Port Bridge, a newly constructed rail-cum-road steel truss bridge in China's Guangdong Province, was selected for a case study.

Based on the geometry and material of the case study bridge, a finite element model was built, and its validity has been confirmed from field testing data. Then fatigue stress response was obtained in the bridge deck under the standard fatigue truck stipulated in Chinese codes. The region around the truss girder was pinpointed as areas of concern (or "hotspots"), which are susceptible to fatigue cracking. As a local structural component, stress at the hotspot is only significant when the wheel loading is within the vicinity of that position. Each passing of a standard fatigue truck causes two cycles of alternating stress. Combining stress due to restrained shrinkage and temperature gradient with the live load effect, deck concrete was found undergoing stress reversals from tension to compression.

The outcome of the fatigue stress analysis then serves as an input for assessing the fatigue performance of the Nansha Port Bridge. Since fatigue design provisions are not available in the Chinese highway concrete bridge code, fib Model Code 2010 was applied for fatigue evaluation of the composite deck. Assessment of fatigue strength, fatigue failure mode, and fatigue life was then performed for the case study bridge.

There are three failure modes for a composite bridge deck under fatigue loading: bending fatigue, direct shear fatigue, and punching shear fatigue. For the Nansha Port Bridge, fatigue life for flexural failure mode is 56 years, the shortest among all failure modes. Bending failure, characterized by fatigue fracture of steel reinforcement, thus becomes the controlling failure mode. Since concrete at the top surface of the bridge deck near the main truss cracks longitudinally as early as after six years of service, the composite bridge deck would perform with cracks during 90% of its life. Therefore, one should carefully consider the cracking resistance of concrete when designing such a bridge deck. Vehicle overloading and understrength of concrete pose additional threats to the fatigue performance of the composite bridge deck.

Although fib Model Code 2010 offers an extensive treatment of fatigue assessment, the level of reliability of different standards may differ. Therefore, it is necessary to research and promote proper design provisions in China's concrete bridge design standard.

We assessed the fatigue performance of the composite bridge deck primarily based on the methods provided by fib Model Code. Refined fatigue evaluation methods may be necessary considering the complexity and uncertainties related to the fatigue load effect, fatigue failure modes, and associated resistance. To study the fatigue failure mechanism of this novice PBL composite bridge deck, an experimental program, including fatigue and fracture tests on both small-sized concrete specimens and large-scale deck panels, is currently undergoing at the Beijing University of Technology.

Acknowledgements This research was funded by the National Natural Science Foundation of China (Grant No. 51008006), and the China Railway No. 18 Engineering Group (No. 40004015201911). We would also like to thank our colleagues Dewang Li and Zhenyu Sun for their contribution in conducting the experimental work.

References

1. Wang C S, Wu Q Y, Miao W H. Fatigue life estimation for reinforced concrete bridge deck. Journal of Chang'an University (Natural Science Edition), 2013, 33(2): 50–55+62 (in Chinese)
2. Collings D. Steel Concrete Composite Bridges. London: Thomas Telford Services Ltd, 2005
3. Li H S. Research on fatigue performance of reinforced concrete carriageway slab and diaphragms of T-beam bridge. Dissertation for the Doctoral Degree. Harbin: Northeast Forestry University, 2019 (in Chinese)
4. Hao C, Cao X L. Application of steel-concrete composite bridge deck in maintenance engineering of highway railway dual-purpose bridge. Engineering and Construction, 2013, 27(6): 853−855 (in

Chinese)
5. Zhao Q, Wu C. Steel Bridge—Steel Structure and Composite Structure Bridge. Beijing: China Communications Press Ltd., 2017 (in Chinese)
6. Abendroth R E, Porter M L. Fatigue behaviour of composite metal deck slabs. Journal of Structural Engineering, 1989, 115(1): 89−103
7. Luo R D, Qu Z F, Wang Z Y, Zhu Z H, Liu Z. Research on mechanical performance of a new type of large longitudinal rib orthotropic-PBL shear connectors composite bridge deck. Journal of Railway Science and Engineering, 2020, 17(11): 2849−2856 (in Chinese)
8. Lu P Z, Zhan X L, Zhao R D. Fatigue behaviour in full-scale laboratory tests of a composite deck slab with PBL reinforcement. Journal of the South African Institution of Civil Engineering, 2017, 59(2): 11−18
9. Ahn J H, Sim C, Jeong Y J, Kim S H. Fatigue behavior and statistical evaluation stress category for a steel-concrete composite bridge deck. Journal of Constructional Steel Research, 2009, 65(2): 373−385
10. Yang Y, Zhou P J, Nie J G, Xie B Y. Experiment on static and fatigue behavior of steel plate-concrete composite bridge decks. China Journal of Highway Transport, 2009, 22(4): 78–83+107 (in Chinese)
11. Li J, Li J, Shao X D,Chen W, Zeng Y. Static and fatigue test on composite deck with steel and ultra-thin UHPC-TPC. China Civil Engineering Journal, 2017, 50(11): 98−106 (in Chinese)
12. Gao Q F, Dong Z L, Cui K M, Liu C, Liu Y. Fatigue performance of profiled steel sheeting-concrete bridge decks subjected to vehicular loads. Engineering Structures, 2020, 213: 110558
13. Huang Q, Zheng H K, Song X D. Experimental study on fatigue performance of GFRP-concrete composite bridge deck. Journal of Highway and Transportation Research and Development, 2019, 36(5): 57–63+77 (in Chinese)
14. Zhao Q, Guo Y B, Chen K S, Lin S S. Influence of ultra-high performance concrete pavement on fatigue performance of steel bridge deck. Journal of Shengyang Jianzhu University (Natural Science), 2019, 35(06): 961−969 (in Chinese)
15. Liu Y M, Zhang Q H, Bao Y, Bu Y. Fatigue behavior of orthotropic composite deck integrating steel and engineered cementitious composite. Engineering Structures, 2020, 220: 111017
16. Zhang H, Zhang Z X, Gao P W, Cui L, Pan Y, Li K. Performance of steel bridge deck pavement structure with ultra-high performance concrete based on resin bonding. Frontiers of Structural and Civil Engineering, 2021, 15(4): 895−904
17. Xu Z Y, Zhao R D, Mu Y M. Experimental study on mechanical behavior of steel-concrete composite bridge deck with PBL connectors. Journal of Building Structures, 2015, 36(S1): 382−388 (in Chinese)
18. Higgins C, Mitchell H. Behavior of composite bridge decks with alternative shear connectors. Journal of Bridge Engineering, 2001, 6(1): 17−22
19. Zhu J S, Zhu X C. Study on simplified method for the analysis of fatigue failure process of RC bridges. Engineering Mechanics, 2012, 29(5): 107–114+121 (in Chinese)
20. Wang Y P, Li J. A review of theoretical study of concrete fatigue. Journal of Tongji University, 2021, 49(5): 617−623
21. Lei J Q, Huang Z W, Gui C Z, Cao S S, Liu H S. Analysis on sustainable development of rail-road bridge. Steel Construction, 2016, 31(11): 1–4+37 (in Chinese)
22. Hu H Y, Liu J F, Ning B W. Design of truss composite girder of bridge of Sanmenxia Huanghe River rail-cum-road bridge. Bridge Construction, 2018, 48(2): 83−88 (in Chinese)
23. Zhu X F. Study on construction optimization and mechanical properties of concrete deck of rail-cum-road steel truss bridge. Thesis for the Master's Degree. Beijing: Beijing University of Technology, 2020 (in Chinese)
24. JTG D60-2015. General Specifications for Design of Highway Bridges and Culverts. Beijing: China Communications Press, 2015 (in Chinese)
25. fib Model Code 2010. fib Model Code for Concrete Structures 2010. Berlin: Wilhelm Ernst & Sohn, 2013
26. Sigrist V, Bentz E, Ruiz M F, Foster S, Muttoni A. Background to the fib model code 2010 shear provisions—Part I: Beams and slab. Structural Concrete, 2013, 14(3): 195−203
27. JTG D40-2011. Specifications for Design of Highway Cement Concrete Pavement. Beijing: China Communications Press, 2011 (in Chinese)
28. Cheng Y K. Analysis of fatigue property and stability of prefabricated steel-concrete composite continuous girder bridges. Thesis for the Master's Degree. Nanjing: Southeast University, 2018 (in Chinese)